Influence of γ–irradiation and ultrasound treatment on carrier transport in Au-SiO_2-Si structure

A.M. Gorb, O.A. Korotchenkov, O.Ya. Olikh*, A.O. Podolian, R.G. Chupryna

Faculty of Physics, Taras Shevchenko National University of Kyiv, Kyiv 01601, Ukraine

Abstract

The effect of ^{60}Co γ–irradiation ($5 \cdot 10^7$ rad) and ultrasound treatment (4 MHz, 2 W/cm^2, up to 60 min) on current–voltage characteristics is experimentally investigated for Au-SiO_2-Si structure. The modification of carrier transport as well as defect subsystem is analysed. In particular, it is shown that irradiation causes the space charge limited current and the trap–assisted tunneling current. Experimental observations of the acoustically induced nearly room–temperature annealing of P_b– and E'—centres and partial recovering of irradiated silicon MOS structure characteristics are highlighted.

Keywords: MOS structures, Si-SiO_2 interface, ultrasound treatment, $\gamma-$rays

1. Introduction

It is well known that the defects are crucial for the semiconductor devices performance. Thus electrical characteristics of metal–oxide–semiconductor (MOS) structure are extremely sensitive to the interface state density. The formation of lattice defects near the interface caused by the irradiation is very harmful for such device performance and leads to the current mechanism change frequently [1–6]. The radiation defects (RDs) are known to be able to effectively interact with elastic acoustic vibrations. E.g. the RDs are annealed by acoustic waves treatment at temperature, which is much lower than ones in the case of ultrasound-free heating. Such phenomenon is observed in the single crystal of Si [7–9], Ge [10] as well as semiconductor [11, 12] and alkaline halide [13] compounds. Usually it deals with a decay of radiation–formed complexes and acoustically induced (AI) diffusion of defects to a sink. Besides, the possibility of parameter recovery of irradiated barrier structures by ultrasound treatment (UST) is shown. So, the active ultrasound effects are observed in the solar cells [14, 15], LEDs [16, 17], and Schottky diodes [18, 19]. The industrially important Si–SiO_2 system is under consideration as well. Particularly, the AI change of

*Corresponding author
Email address: olikh@univ.kiev.ua (O.Ya. Olikh)

the Si–SiO_2 interface defects [20–22] and minority carrier lifetime [23–25] are reported.

Some attention is paid to the UST of silicon MOS structures, which have been irradiated by ^{60}Co γ–rays [26, 27]. The decrease of the both radiation–induced charge in the dielectric layer and generation lifetime in the silicon, and the insignificant growth of the surface recombination rate after UST have been determined by capacitancevoltage characteristics measurements [26, 27].

The first aim of our work is to investigate experimentally the UST influence on a charge transfer in the irradiated Au–SiO_2–Si structures. In contrast to the cited study [26, 27], our results are obtained i) for systems with a significantly higher RD concentration (see Section 2); ii) for operating mode of diode, that is, when the current was present. It should be noted that our some result was reported previously [25]. But this work is focused on the modification of charge transfer mechanisms as well as the defect structure due to irradiation and UST.

On the other hand, in the silicon solar cell industry, the efficiency of a cell is restricted by the recombination of carriers [28]. The silicon surface is often highly recombination active due to the abundance of band–gap states that exist due to dangling bonds. The number of band–gap states can be reduced by introducing a dielectric coating. The alneal is one of the most effective methods of passivating the Si–SiO_2 interface [28–30]. This reaction is reported to release atomic hydrogen that is then free to diffuse across the oxide and passivate dangling bonds at the oxide–silicon interface [29–31]. In this work, it is demonstrated that it is possible to enhance the hydrogen diffusion by ultrasound. Therefore, acousto–alneal can be effective processing step.

2. Experimental and calculation details

Experiments were performed on n-type (111)–oriented crystalline float-zone Si with residual boron (B) impurity concentration of about 10^{12} cm^{-3} and doping phosphorus (P) impurity concentration of $2 \cdot 10^{12}$ cm^{-3}. The corresponding resistivity is 4000 Ω·cm. A bulk silicon material was divided into several rectangular–shaped samples of approximately $1 \times 5 \times 10$ mm^3. The MOS structures were formed by chemical etching of the upper Si surfaces using HF-HNO_3–CH_3COOH solutions (HF:HNO_3:CH_3COOH = 3 : 5 : 3), followed by the surface oxidation due to the exposure to ambient air for 24 hours and the Au vacuum evaporation. GaZn–eutectic Ohmic contacts were rubbed on the bottom surfaces of the samples.

The samples were γ–irradiated (^{60}Co source) at nominal room temperature to the dose $5 \cdot 10^7$ rad. The measurement on the reference bulk sample shown that the conductivity has been reduced to about 0.5 of the initial value after irradiation. As it was mentioned above, the ultrasonical recovering of the γ–irradiated silicon MOS structures has been investigated [26, 27] early. The structures Si–SiO_2, which have been produced by thermal oxidation of silicon, were under consideration [26, 27] as well. But the more heavy degradation and the higher RD concentration were expected in the our case. The main reasons are following. i) The high doze was used ($5 \cdot 10^7$ rad in our case as against 10^6 rad in [26, 27] case). ii) The semiconductor resistivity was greater (4000 Ω·cm as against $0.2 - 0.5$ Ω·cm); therefore the non–ionizing energy losses was larger as well. iii) It is known [32], that the surface defect density, which is γ–induced in Si–SiO_2, is about 10^{12} eV/cm for 10^7 rad in the case of (111)–oriented substrate and this value is much more then one for (100)–substrate, which is used in cited study.

The UST of the irradiated structure was done by attaching the piezoelectric transducer to one side of the sample. An epoxy glue was used as the bondingmedium, providing the rigid coupling of the transducer to the sample. The thickness resonant of the transducers was 4 MHz. A radio–frequency voltage supplied from a generator drives the transducer, resulting in vibrations of the coupled transducer-sample system. UST was carried out by a two consecutive loading–unloading cycles, 30 min each; so the total UST time t_{UST} was equal to 30 min or 60 min. The density of acoustic energy flux W_{US} in Si was equal to about 2 W/cm^2. The sample temperature was measured with a copper–constantan thermocouple directly attached to the surface and did not exceed 350 K. The more details about the sample and UST setup are presented elsewhere [25].

The characteristics of the Au-SiO_2-Si structure, after γ–irradiation and after UST, were investigated using an current–voltage ($I-V$) technique. The forward and reverse bias characteristics were measured in current range from 10^{-9} to 10^{-3} A with a voltage step of 0.01 V at 295 K.

The data non–linear fitting were done by using the method of modified artificial bee colony [33].

3. Results and Discussion

Fig. 1 shows IV characteristics for both initial and irradiated Au–SiO_2–Si structure as well as after the sequent USTs. One can see that IV characteristic for non-irradiated sample is typical for Schottky diode: the forward current is caused by a thermionic emission (TE) over barrier, the reverse current value is determined by barrier height lowering, which occur due to the electric field ($\log I \sim V^{1/2}$) [34, 35]. The forward branch was fitted by the following equation [34]

$$I = I_s \left\{ \exp\left[\frac{q(V - IR_s)}{nkT}\right] - 1 \right\} , \tag{1}$$

where I_s is the saturation current, R_s is the series resistance, n is the ideality factor, the other symbols have their usual meanings. The fitting results are shown on Fig. 1(b) and (d) by solid lines, the obtained parameters values are listed in Table 1. It should be noted that the oxide layer presence does not allow to determinate the barrier height by help the saturation current value only, since the tunneling must be taken into account as well [36, 37].

In addition, the real current value for the non-irradiated structure exceeds one, which is expected from Eq. (1) — see Fig. 1. The redundant current is

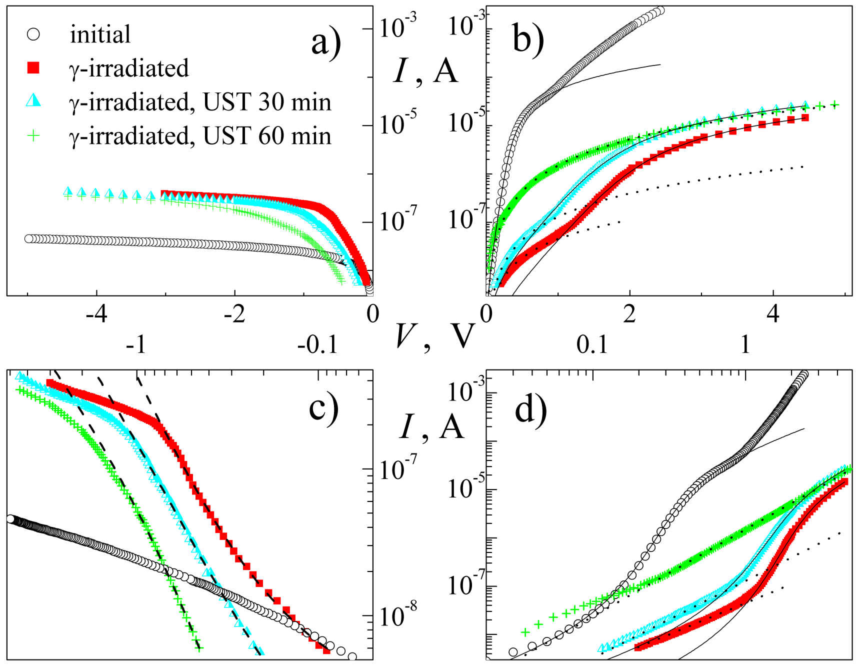

Figure 1: The logarithmical (a, b) and double-logarithmical (c, d) plots of the reverse (a, c) and forward $I-V$ characteristics for Au–SiO_2–Si structure before and after γ–irradiation and UST. $T = 300$ K. The marks are the experimental results, and the solid, dashed, and dotted lines are the TE, TAT, and SCLC fitted curves using Eq. (1), (7), and (3) correspondingly.

Table 1: Extracted parameters for the Au–SiO_2–Si structure

Structure status				
γ–irradiation	–	+	+	+
UST	–	–	+	+
t_{UST} (min)	0	0	30	60
Parameter				
I_s (10^{-9}A)	3.3 ± 0.3	1.1 ± 0.2	4.9 ± 0.5	–
R_s (10^4)	1.1 ± 0.2	13 ± 1	9 ± 1	–
n	1.7 ± 0.1	10.3 ± 0.2	9.9 ± 0.2	
m_{F}	–	1.30 ± 0.05	1.6 ± 0.05	1.8 ± 0.05
I_0 (10^{-8}A)	–	5 ± 1	13 ± 2	150 ± 10
$I_{0,\mathrm{TAT}}$ (a.u.)	–	1	0.14 ± 0.03	0.04 ± 0.01
U_d (V)	–	0.7 ± 0.1	0.44 ± 0.05	0.12 ± 0.05
R_{TAT} (a.u.)		1	0.54 ± 0.05	0.33 ± 0.04
$K_{\mathrm{RECT,\ 0.5V}}$	800 ± 100	0.22 ± 0.03	1.3 ± 0.2	5.4 ± 0.8

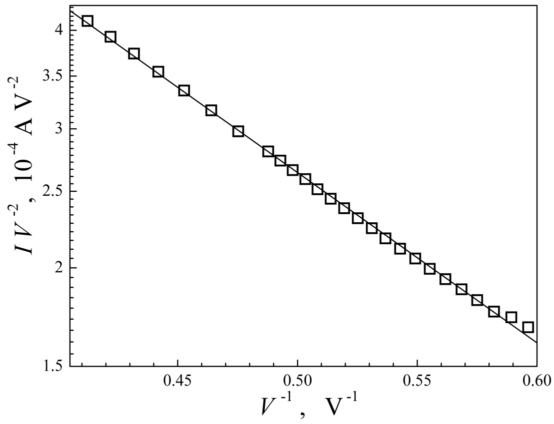

Figure 2: The Fowler-Nordheim plot of the forward branch for non–irradiated Au–SiO_2–Si structure at $V > 1,6$ V. The line is the least–squares linear fitting.

most likely to be caused by the tunneling through the SiO_2 layer and can be described as [34, 38]:

$$\ln\left(\frac{I}{F_m^2}\right) \propto -\frac{4\sqrt{2m^*}(qE_{\rm eff})^{3/2}}{3\hbar q F_m}\,, \tag{2}$$

where F_m is the electric field, $E_{\rm eff}$ is the effective tunneling energy. The linearity of the Fowler–Nordheim plot of the forward current at large bias is this assumption evidence — see Fig. 2. It was taken into account when plotting that the electric field in a oxide layer is proportional to the applied voltage $F_m \propto V$.

As shown in Fig. 1, the γ–irradiation has a considerable effect on the current behavior. The changes are pronounced for the reverse branch especially and the $I - V$ characteristic modification is the evidence of a transformation of the current transport mechanism. Thus the forward $I - V$ dependence, expected according to TE model, is observed at $V > 1$ V only and the current value is much more then one in the non–irradiated case. The fitting of the $V > 1$ V region by Eq. (1) shows that the irradiation leads to significant increase in both series resistance and ideality factor values — see Table 1 data. And the former significantly exceeds the resistance change, which has been observed in the bulk samples. The ideality factor increase deals with the RDs formation and results in the observed TE current decreasing. Note that the effect of the radiation induced decreasing of MOS structure current is known [39].

Pintilie, *et al.* [40] have investigated the RD formation by ^{60}Co γ-radiation in silicon. The both growth method and resistivity have been analogous to structure under our investigation and the dose $9 \cdot 10^7$ rad has been used. It has been shown that complexes VO_i, ${}_i\mathrm{C}_s$, H–centre ($\mathrm{V_2O}_i$), Γ–centre, and interstitial defect $I^{0/-}$ are the main radiation defects. The latest one is a secondary defect and its appearance leads to a conductivity compensation (inversion) [40].

In our case the series resistance change in a range one order of magnitude above causes the reduction of voltage drop in the dielectric layer. As a result, the electric field intensity was ceased to be sufficient for effective Fowler–Nordheim tunneling and the corresponding current component was not observed after irradiation.

Fig. 1(d) shows that the forward $I-V$ characteristic of irradiated structures at low biases ($V < 1$ V) is enough good described by a power law

$$I = I_0 \, V^{\,m_{\mathrm{F}}}, \tag{3}$$

where $m_{\mathrm{F}} = \frac{V}{I}\frac{\partial V}{\partial I}$ is the power–law parameter. The relation (3) is typical for the space charge limited current (SCLC) [41–43] and the m_{F} value is connected with the energy distribution of traps, which emit carriers. E.g. the value $m_{\mathrm{F}} \approx 1,3$, which is observed for the investigated structure after γ–irradiation and before UST, is evident of the exponentially distributed traps. It is known [41–43] that the I_0 depends on the total trap concentration N_t

$$I_0 \sim 1/N_t^{m_{\mathrm{F}}-1}, \tag{4}$$

and the temperature dependency of power–law parameter is defined by equation

$$m_{\mathrm{F}} = 1 + T_c/T, \tag{5}$$

where T_c is the characteristic temperature parameter of the trap distribution; notably the trap concentration per unit energy range at an energy E above the valence band is proportional to $\exp(-E/kT_c)$.

The SCLC current-voltage relation is often written as [42]

$$I(V,T) = C \exp\left(-\frac{E_x}{kT}\right) V^{\,m_{\mathrm{F}}(T)}, \tag{6}$$

where C is the constant, E_x is the activation energy that defined by the level position of the filled traps to the conductivity band. Fig. 3 shows the temperature dependence of the forward current. Eq. (5) was taken into account when Fig. 3 plotting. One can see that the experimental data are in good agreement with the fitting curve by Eq. (6) for value $E_x = (0,32 \pm 0,01)$ eV.

The γ–irradiation of Si–SiO_2 structures is known [32] to lead to a mechanical stress relaxation, a trap filling, and a new charged defect generation. It is believed [44, 45] that the negative charge is trapped at the interface while the positive charge accumulates at E'–centers, E'_δ–centers, and three strained bond related centers. However, the E' and E'_δ concentration considerably overrides the bond related centers concentration in the case of defect formation by photons (X– and γ–rays) [44]. It should be noted that the low temperature as well as low partial oxygen pressure result in the thin SiO_2 layer formation in the structure under investigation. But it is known [46] that RDs, which appear in thin and thick layers, are the same.

Note that the hydrogen content is the key factor of a generation of the electrically active RDs in silicon MOS structures [46] and the SiO_2 layers, which are grown by thermal oxidation, are rich in an atomic hydrogen [32]. The

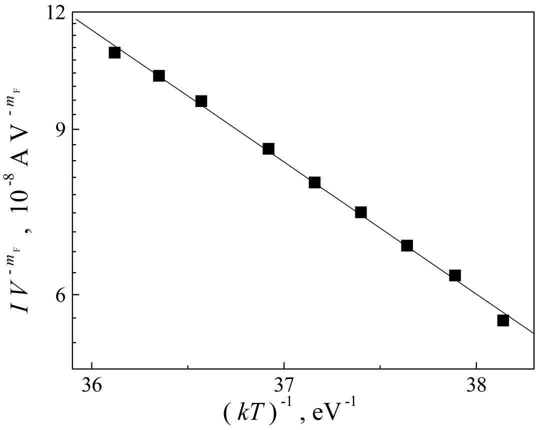

Figure 3: Temperature dependence of SCLC–current for γ–irrradiated Au–SiO_2–Si structure before UST at $V = 0,4$ V. The line is the least–squares linear fitting.

irradiation is known [47, 48] to lead to the breaking of $\equiv \mathrm{Si}-\mathrm{H}$ bonds at the Si–SiO_2 interface and subsequent diffusion of released H species into the oxide bulk. The resulting unsaturated bonds $\equiv \mathrm{Si}-$ act as electronic traps. Generally such defects are distinguished by the orientation of the silicon substrate. It is considered [49] that P_b centers appear at (111)–oriented substrate interface whereas P_{b1} and P_{b0} centers are typical in the case of (100)–oriented substrate. Both P_{b0} and P_{b1} are chemically identical to the P_b center, however the difference in an electrical activity is observed [49].

The non–monotonic energy distribution of the interface levels is observed in Si–SiO_2 structures, grown on n–type silicon crystal, after the γ–rays irradiation with dose above $5 \cdot 10^5$ rad [32]. According to Parchinskii, *et al.* [50], the highest density of surface states is observed at $E_c - (0,32 \pm 0,04)$ eV. This value coincides with the determined E_x value. Therefore the current at low forward bias for irradiated structures deals with carriers, which are trapped by P_b–centers. Besides the negative charge accumulation at interface results in both barrier height increase and observed TE current decreasing. But as mentioned above, the main reason of TE current reduction is the n rise, which is induced by RDs generation at silicon near surface region.

As shown in panel (b) and (d) of Fig. 1, USTs cause an increase of a space charge limited current. In particular, SCLC exceeds the TE current at the whole used forward voltage interval in the case of $t_{\mathrm{UST}} = 60$ min. We used Eq. (3) to fit experimental $I-V$ data of irradiated and ultrasonically treated structures. The obtained fitting parameters are summarized in Table 1. According to Eq. (4), the detected increase in I_0 value is evident of AI decrease in P_b–center concentration. It was experimentally observed that the acousto-defect interaction in Si structures mainly cause atomic diffusion, transformation of native and impurity defects, modification of interior surface states, and appearance of new defects [21, 51–55]. But the P_b–center annealing is known [56, 57] to deal with the passivation of dangling bonds at the oxide–silicon interface by hydrogen atoms. Thus the obtained results indicate about the AI diffusion of hydrogen. Similar process has been reported early [20, 58, 59], but the RDs acoustically–induced annealing was observed in our case.

The AI increase in m_{F} value (or T_c rising — see Eq. (5)) testifies to the narrowing of the trap level energy distribution. So it is known [42] that $m_{\mathrm{F}} = 2$ is observed in the case of single–energy trap. The detected narrowing of the energy distribution is evident of a AI passivation selectivity, that is, UST leads to atomic hydrogen capture by dangling bonds, which correspond to certain levels only. In our opinion, the key parameter of the bond ultrasound passivation is a mechanical stress, which are generally non–uniform at the interface. The impurity diffusivity is known [60] to depend on mechanical stress. On the one hand, it can be a reason of a hydrogen displacement under acoustic loading condition. On the other hand, the effectiveness of AI passivation is determined by a mechanical deformation level and UST assists to the structure uniformity.

AI bond passivation lead to a decrease in interface negative charge, which is trapped by P_b–centers; as a consequence, a partial recovery of barrier height and a TE current increase are observed — see I_s data in Table 1. The detected decrease in the series resistance value after UST is evidence of the RDs annealing in the semiconductor bulk.

The hydrogen released during the irradiation is potentially hazardous because of this mobile species can then [44, 47, 48, 61] i) interact with other bonded hydrogen at $\mathrm{Si/SiO_2}$ interface and give rise to additional P_b–centers; ii) move to semiconductor bulk and produce generation–recombination sites and boron deactivation in the Si substrate; iii) migrate within the oxide and results in the creation of the bulk–oxide traps E'–centers, which is believed to be due to broken $\equiv \mathrm{Si}-\mathrm{O}$ bonds. The E'—centre is a defect resulting from an oxygen vacancy in $\mathrm{SiO_2}$ and traps positive charge [44, 56]. The E' total concentration is about 10^{18} cm^{-3} in the case of 10^7 rad γ–irradiation, but centers are non–uniformly distributed over oxide layer and largest concentration are expected near $\mathrm{Si/SiO_2}$ interface. The broken $\equiv \mathrm{Si}-\mathrm{O}$ bonds are not known to recover at room temperature and the E' annealing temperature is equal $(200\div400)^{\circ}$C [47].

E'—centres at oxide bulk give rise to stress–induced leakage current (SILC)[47, 61]. It is precisely this current that is observed in the irradiated structure under reverse bias — see panels (a) and (c) on Fig. 1. In fact, the conduction mechanism responsible for SILC is generally assumed [48, 61] to be a trap–assisted tunneling (TAT). According to [62–64], the field dependence of TAT current is described as

$$I_R = I_{0,\mathrm{TAT}}\,(U_d + V)\exp\left(-\frac{R_{\mathrm{TAT}}}{F_m}\right), \tag{7}$$

where $I_{0,\mathrm{TAT}}$ and R_{TAT} do not depend on voltage, $I_{0,\mathrm{TAT}}$ is proportional to trap concentration, U_d is the barrier height. The measured reverse $I-V$ branches were fitted by using Eq. (7). It has been found that the experimental data are in good agreement with the fitting curves (see Fig. 1) for values, listed in

Table 1. This confirms assumptions about the reverse current mechanism in the irradiated structures. The current deviations at high bias probably caused by series resistance.

Table 1 data illustrate that USTs lead to decrease in $I_{0,\mathrm{TAT}}$ and barrier height values. The former is evidence of low temperature (about 80°C) AI annealing of radiation traps. In our opinion, the E'–centers annealing is caused by acoustically stimulated diffusion of interstitial oxygen atoms.

UST of γ–irradiated Au-SiO_2-Si structure leads to a forward current increase as well reverse current decrease. Therefore the rectification factor K_{RECT}, that has became considerably degraded after irradiation, was recovered by an acoustic wave action. The K_{RECT} data at 0.5 V are listed in Table 1. Thereby in this work, it is demonstrated that it is possible to partially recovery the quality of γ–degraded silicon MOS structure by nearly room–temperature ultrasound treatment.

4. Conclusion

The experimental investigation of influence of γ–irradiation and ultrasound treatment on carrier transport in Au-SiO_2-Si structure has been carried out. It has been shown that γ–irradiation gives rise the space charge limited current and the trap–assisted tunneling current at forward and reverse bias, respectively. The investigation has revealed that ultrasound treatment leads to nearly room–temperature annealing of radiation defects (P_b–centers and E'—centres) and partially recovery of silicon MOS structure characteristics. The acoustically induced annealing is caused by the enhance of a diffusivity of interstitial species (hydrogen and oxygen) under ultrasound loading condition. By relying on increase in the value of power–law parameter of a space charge limited current, it has been concluded that ultrasound treatment leads to narrowing of energy distribution of γ–induced traps at Si/SiO_2 interface. Thus, ultrasound can be an effective tool for controlling metal-semiconductor structure characteristics.

References

[1] A. Rao, S. Krishnan, G. Sanjeev, K. Siddappa, Effect of 8 Mev Electrons on Au/n–Si Schottky diodes, Int. J. Pure Appl. Phys. 5 (1) (2009) 55–62.

[2] lke Taolu, A. Tatarolu, A. zbay, emsettin Altndal, The role of ^{60}Co γ–ray irradiation on the interface states and series resistance in MIS structures, Radiat. Phys. Chem. 79 (4) (2010) 457–461. doi:10.1016/j.radphyschem.2009.10.002.

[3] A. Tatarolu, . Antindal, Analysis of interface states and series resistance at MIS structure irradiated under ^{60}Co $\gamma-$rays, Nucl. Instrum. Methods Phys. Res., Sect. A 580 (3) (2007) 1588–1593. doi:10.1016/j.nima.2007.07.027.

[4] O. Y. Olikh, Non-monotonic $\gamma-$ray influence on Mo/n-Si Schottky barrier structure properties, IEEE Trans. Nucl. Sci. 60 (1) (2013) 394–401. doi:10.1109/TNS.2012.2234137.

[5] S. Verma, K. C. Praveen, A. Bobby, D. Kanjilal, Recovery of electrical characteristics of au/n-si schottky junction under ^{60}Co gamma irradiation, IEEE Transactions on Device and Materials Reliability 14 (2) (2014) 721–725. doi:10.1109/TDMR.2014.2312753.

[6] M. A. Salari, B. Gzeldir, M. Salam, The effects of gamma irradiation on electrical characteristics of zn/zno/n-si/au-sb structure, AIP Conference Proceedings 1935 (1) (2018) 050002. doi:10.1063/1.5025974.

[7] A. O. Podolian, A. B. Nadtochiy, O. A. Korotchenkov, Charge carrier lifetime recovery in $\gamma-$irradiated silicon under the action of ultrasound, Tech. Phys. Lett. 38 (5) (2012) 405–408. doi:10.1134/S1063785012050124.

[8] A. Podolyan, V. Khivrich, Room–temperature ultrasonic annealing of radiation defects in silicon, Tech. Phys. Lett. 31 (10) (2005) 11–16. doi:10.1134/1.1931783.

[9] Y. Olikh, M. Tymochko, A. Dolgolenko, Acoustic–wave–stimulated transformations of radiation defects in $\gamma-$irradiated n–type silicon crystals, Tech. Phys. Lett. 32 (7) (2006) 586–589. doi:10.1134/S106378500607011X.

[10] Y. Olikh, N. Karas', On the effect of ultrasound on the annealing of radiation defects in neutron-doped germanium, Fizika i tekhnika poluprovodnikov 30 (8) (1996) 1455–1459.

[11] Y. Olikh, V. Tartachnik, I. Tichyna, V. R.M., Termoacoustic annealing of radiation–induced defects in indium–phosphide crystal, in: The proceeding of 5th conference "Acoustoelectronics 91", 1991, pp. 95–96, Varna, Bulgaria.

[12] I. Ostrovskii, O. Korotchenkov, V. A. Lysyh, Annealing of point defects by ultrasound in solids, Soviet Physics Solid State 20 (7) (1987) 2153–2156.

[13] I. Ostrovskii, N. Ostrovskaya, O. Korotchenkov, J. Reidy, Radiation defects manipulation by ultrasound in ionic crystals, IEEE Trans. Nucl. Sci. 52 (6) (2005) 3068–3073. doi:10.1109/TNS.2005.861476.

[14] N. Guseynov, Y. Olikh, S. Askerov, Ultrasonic treatment restores the photoelectric parameters of silicon solar cells degraded under the action of ^{60}Co gamma radiation, Tech. Phys. Lett. 33 (1) (2007) 18–21. doi:10.1134/S1063785007010063.

[15] O. Y. Olikh, A. M. Gorb, R. G. Chupryna, O. V. Pristay-Fenenkov, Acousto–defect interaction in irradiated and non–irradiated silicon n^{+}–p structure, J. Appl. Phys. 123 (16) (2018) 161573. doi:10.1063/1.5001123.

[16] O. Konoreva, M. Lytovchenko, Y. Malyi, Y. Olikh, I. Petrenko, M. Pinkovska, V. Tartachnyk, Acoustic–stimulated relaxation of gaas$_{1-x}$p$_x$ leds electroluminescence intensity, Semiconductor Physics, Quantum Electronics & Optoelectronics 19 (1) (2016) 34–38. doi:10.15407/spqeo19.01.034.

[17] O. Konoreva, Y. M. Olikh, M. Pinkovska, O. Radkevych, V. Tartachnyk, V. Shlapatska, The influence of acoustic–dislocation interaction on intensity of the bound exciton recombination in initial and irradiated gaasp leds structures, Superlattices Microstruct. 102 (2017) 88–93. doi:10.1016/j.spmi.2016.12.026.

[18] I. G. Pashaev, Study of the relaxation of the excess current in silicon schottky diodes, Semiconductors 48 (10) (2014) 1391–1394. doi:10.1134/S1063782614100224.

[19] O. Olikh, Reversible influence of ultrasound on $\gamma-$irradiated Mo/n-Si Schottky barrier structure, Ultrasonics 56 (2015) 545–550. doi:10.1016/j.ultras.2014.10.008.

[20] S. Ostapenko, L. Jastrzebski, J. Lagowski, R. K. Smeltzer, Enhanced hydrogenation in polycrystalline silicon thin films using low–temperature ultrasound treatment, Appl. Phys. Lett. 68 (20) (1996) 2873–2875. doi:10.1063/1.116353.

[21] D. Kropman, V. Seeman, S. Dolgov, A. Medvids, Effect of ultrasonic treatment on the defect structure of the Si–SiO$_2$ system, Phys. Status Solidi C 13 (10–12) (2016) 793–797. doi:10.1002/pssc.201600052.

[22] N. Zaveryukhina, E. Zaveryukhina, S. Vlasov, B. Zaveryukhin, Acoustostimulated changes in the density of surface states and their energy spectrum in p–type silicon single crystals, Tech. Phys. Lett. 34 (3) (2008) 241–243. doi:10.1134/S106378500803019X.

[23] P. Parchinskii, S. Vlasov, L. Ligai, O. Y. Shchukina, The effect of ultrasonic treatment on the generation characteristics of a Si–SiO$_2$ interface, Tech. Phys. Lett. 29 (5) (2003) 392–394. doi:10.1134/1.1579804.

[24] A. Zbelskyy, D. Kropman, S. M.K., The effect of ultrasound on point defects in structures Si–Sio$_2$, Zhurnal tekhnicheskoy fiziki 59 (8) (1989) 131–134.

[25] A. Gorb, O. Korotchenkov, O. Olikh, A. Podolian, Ultrasonically recovered performance of $\gamma-$irradiated metal-silicon structures, IEEE Trans. Nucl. Sci. 57 (3) (2010) 1632–1639. doi:10.1109/TNS.2010.2047655.

[26] P. B. Parchinskii, S. I. Vlasov, R. A. Muminov, K. K. Ismailov, U. Turgunov, The effect of ultrasound on the parameters of metal–dielectric–semiconductor structures, Tech. Phys. Lett. 26 (10) (2000) 420–422. doi:10.1134/1.1262865.

[27] P. Parchinskii, S. Vlasov, L. Ligai, Effect of ultrasonic treatment on the generation characteristics of irradiated silicon–silicon–dioxide interface, Semiconductors 40 (7) (2006) 808–811. doi:10.1134/S106378260607013X.

[28] K. A. Collett, R. S. Bonilla, P. Hamer, G. Bourret-Sicotte, R. Lobo, T. Kho, P. R. Wilshaw, An enhanced alneal process to produce SRV $<$ 1cm/s in 1ω cm n–type Si, Sol. Energy Mater. Sol. Cells 173 (2017) 50–58. doi:10.1016/j.solmat.2017.06.022.

[29] M. J. Kerr, A. Cuevas, Very low bulk and surface recombination in oxidized silicon wafers, Semiconductor Science and Technology 17 (1) (2001) 35–38. doi:10.1088/0268-1242/17/1/306.

[30] A. G. Aberle, Surface passivation of crystalline silicon solar cells: a review, Prog. Photovoltaics Res. Appl. 8 (5) (2000) 473–487. doi:10.1002/1099-159X(200009/10)8:5¡473::AID-PIP337¿3.0.CO;2-D.

[31] Y. Larionova, V. Mertens, N.-P. Harder, R. Brendel, Surface passivation of n–type Czochralski silicon substrates by thermal–SiO_2/plasma–enhanced chemical vapor deposition SiN stacks, Appl. Phys. Lett. 96 (3) (2010) 032105. doi:10.1063/1.3291681.

[32] V. Pershenkov, V. Popov, A. Shalnov, Poverkhnostnye radiatsiyni efekty v elementakh intehralnykh mikroskhem, Enerhoatomyzdat, Moskow, 1988.

[33] N. Karaboga, S. Kockanat, H. Dogan, The parameter extraction of the thermally annealed schottky barrier diode using the modified artificial bee colony, Appl. Intell. 38 (3) (2013) 279–288. doi:10.1007/s10489-012-0372-x.

[34] E. H. Rhoderick, R. H. Williams, Metal–Semiconductor Contacts, 2nd Edition, Clarendon Press, Oxford, 1988.

[35] J. Andrews, M. Lepselter, Reverse current-voltage characteristics of metal-silicide Schottky diodes, Solid-State Electron. 13 (7) (1970) 1011–1023. doi:10.1016/0038-1101(70)90098-5.

[36] A. M. Ozbek, B. J. Baliga, Tunneling coefficient for GaN Schottky barrier diodes, Solid-State Electron. 62 (1) (2011) 1–4. doi:10.1016/j.sse.2011.04.016.

[37] H. Kobayashi, T. Ishida, Y. Nakato, H. Mori, Mechanism of carrier transport through a silicon–oxide layer for indium–tin–oxide/silicon–oxide/silicon solar cells, J. Appl. Phys. 78 (6) (1995) 3931–3939. doi:10.1063/1.359912.

[38] Y. N. Novikov, Non-volatile memory based on silicon nanoclusters, Semiconductors 43 (8) (2009) 1040–1045. doi:10.1134/S1063782609080144.

[39] G. Niu, G. Banerjee, J. D. Cressler, J. M. Roldan, S. D. Clark, D. C. Ahlgren, Electrical probing of surface and bulk traps in proton-irradiated gate–assisted lateral PNP transistors, IEEE Trans. Nucl. Sci. 45 (6) (1998) 2361–2365. doi:10.1109/23.736455.

[40] I. Pintilie, E. Fretwurst, G. Lindstrm, J. Stahl, Second–order generation of point defects in gamma–irradiated float-zone silicon, an explanation for "type inversion", Appl. Phys. Lett. 82 (13) (2003) 2169–2171. doi:10.1063/1.1564869.

[41] D.-H. Ma, W.-J. Zhang, R.-Y. Luo, Z.-Y. Jiang, Qiang-Ma, X.-B. Ma, Z.-Q. Fan, D.-Y. Song, L. Zhang, Effect of si nanoparticles on electronic transport mechanisms in p-doped silicon-rich silicon nitride/c-si heterojunction devices, Mater. Sci. Semicond. Process. 50 (2016) 20–30. doi:10.1016/j.mssp.2016.04.001.

[42] M. M. A.-G. Jafar, High-bias current–voltage–temperature characteristics of undoped rf magnetron sputter deposited boron carbide (B_5C)/p–type crystalline silicon heterojunctions, Semicond. Sci. Technol. 18 (1) (2003) 7–22. doi:10.1088/0268-1242/18/1/302.

[43] M. Kaya, H. etin, B. Boyarbay, A. Gk, E. Ayyildiz, Temperature dependence of the current–voltage characteristics of sn/pani/p—si/al heterojunctions, J. Phys.: Condens. Matter 19 (40) (2007) 406205. doi:10.1088/0953-8984/19/40/406205.

[44] R. A. B. Devine, The structure of SiO_2, its defects and radiation hardness, IEEE Trans. Nucl. Sci. 41 (3) (1994) 452–459. doi:10.1109/23.299784.

[45] P. M. Lenahan, J. F. Conley, What can electron paramagnetic resonance tell us about the Si/SiO_2 system?, J. Vac. Sci. Technol. B 16 (4) (1998) 2134–2153. arXiv:https://avs.scitation.org/doi/pdf/10.1116/1.590301, doi:10.1116/1.590301.

[46] J. L. Cantin, H. J. von Bardeleben, J. L. Autran, Irradiation effects in ultrathin Si/SiO_2 structures, IEEE Trans. Nucl. Sci. 45 (3) (1998) 1407–1411. doi:10.1109/23.685215.

[47] S. Mahapatra, D. Saha, D. Varghese, P. B. Kumar, On the generation and recovery of interface traps in MOSFETs subjected to NBTI, FN, and HCI stress, IEEE Trans. Electron Devices 53 (7) (2006) 1583–1592. doi:10.1109/TED.2006.876041.

[48] D. Esseni, J. D. Bude, L. Selmi, On interface and oxide degradation in VLSI MOSFETs. i. deuterium effect in CHE stress regime, IEEE Trans. Electron Devices 49 (2) (2002) 247–253. doi:10.1109/16.981214.

[49] D. K. Schroder, J. A. Babcock, Negative bias temperature instability: Road to cross in deep submicron silicon semiconductor manufacturing, J.

Appl. Phys. 94 (1) (2003) 1–18. arXiv:https://doi.org/10.1063/1.1567461, doi:10.1063/1.1567461.

[50] P. B. Parchinskii, S. I. Vlasov, A. Nasirov, The effect of γ–ray radiation on the characteristics of the interface between silicon and lead–borosilicate glass, Semiconductors 38 (11) (2004) 1304–1307. doi:10.1134/1.1823064.

[51] M. Jivanescu, A. Romanyuk, A. Stesmans, Influence of in suti applied ultrasound during Si^+ implantation in Sio_2 on paramagnetic defect generation, J. Appl. Phys. 107 (11) (2010) 114307. doi:10.1063/1.3369041.

[52] O. Korotchenkov, H. Grimmliss, Long-wavelength acoustic-mode-enhanced electron emission from Se and Te donors in silicon, Phys. Rev. B 52 (20) (1995) 14598–14606. doi:10.1103/PhysRevB.52.14598.

[53] O. Y. Olikh, The variation in activity of recombination centers in silicon p–n structures under the conditions of acoustic loading, Semiconductors 43 (6) (2009) 745–750. doi:10.1134/S1063782609060116.

[54] O. Y. Olikh, K. V. Voytenko, R. M. Burbelo, Ultrasound influence on I–V–T characteristics of silicon Schottky barrier structure, J. Appl. Phys. 117 (4) (2015) 044505. doi:10.1063/1.4906844.

[55] R. Savkina, A. Smirnov, T. Kryshtab, A. Kryvko, Sonosynthesis of microstructures array for semiconductor photovoltaics, Mater. Sci. Semicond. Process. 37 (2015) 179–184. doi:10.1016/j.mssp.2015.02.066.

[56] K. Takakura, H. Ohyama, A. Ueda, M. Nakabayashi, K. Hayama, K. Kobayashi, E. Simoen, A. Mercha, C. Claeys, Recovery behaviour resulting from thermal annealing in n–MOSFETs irradiated by 20 MeV protons, Semicond. Sci. Technol. 18 (6) (2003) 506–511. doi:10.1088/0268-1242/18/6/319.

[57] H. Wurzer, R. Mahnkopf, H. Klose, Annealing of degraded npn–transistors-mechanisms and modeling, IEEE Trans. Electron Devices 41 (4) (1994) 533–538. doi:10.1109/16.278506.

[58] J. Koshka, S. Ostapenko, T. Ruf, J. M. Zhang, Activation of luminescence in polycrystalline silicon thin films by ultrasound treatment, Appl. Phys. Lett. 69 (17) (1996) 2537–2539. arXiv:https://doi.org/10.1063/1.117731, doi:10.1063/1.117731.

[59] S. S. Ostapenko, Mechanism of ultrasonic enhanced hydrogenation in poly–Si thin films, in: Defects in Semiconductors 19, Vol. 258 of Materials Science Forum, Trans Tech Publications, 1997, pp. 197–202. doi:10.4028/www.scientific.net/MSF.258-263.197.

[60] M. J. Aziz, Stress effects on defects and dopant diffusion in Si, Mater. Sci. Semicond. Process. 4 (5) (2001) 397–403. doi:10.1016/S1369-8001(01)00014-2.

[61] D. J. DiMaria, E. Cartier, Mechanism for stress–induced leakage currents in thin silicon dioxide films, J. Appl. Phys. 78 (6) (1995) 3883–3894. arXiv:https://doi.org/10.1063/1.359905, doi:10.1063/1.359905.

[62] A. S. Gilmore, J. Bangs, A. Gerrish, I–v modeling of current limiting mechanisms in hgcdte fpa detectors, Proc.SPIE 5563 (2004) 46–54. doi:10.1117/12.562614.

[63] V. Gopal, S. K. Singh, R. M. Mehra, Excess dark currents in hgcdte p^+–n junction diodes, Semicond. Sci. Technol. 16 (5) (2001) 372–376. doi:10.1088/0268-1242/16/5/316.

[64] V. Gopal, A new approach to investigate leakage current mechanisms in infrared photodiodes from illuminated current–voltage characteristics, J. Appl. Phys. 116 (8) (2014) 084502. doi:10.1063/1.4893899.